Electronic Supplementary Material (ESI) for Dalton Transactions.
This journal is © The Royal Society of Chemistry 2019

Coordination-induced metal-to-macrocycle charge transfer and effect of cations on reorientation of CN ligand and geometry of Pc macrocycle in the $\{SnL_2Mac\}^{2-}$ dianions (L= CN^-, OCN^-, Im^-, Mac = phthalo- or naphthalocyanine).

Dmitri V. Konarev,*[a] Alexey V. Kuzmin,[b] Alexander F. Shestakov,[a] Salavas S. Khasanov,[b] Rimma N. Lyubovskaya[a]

[a]Institute of Problems of Chemical Physics RAS, Chernogolovka, Moscow region, 142432 Russia;

[b]Institute of Solid State Physics RAS, Chernogolovka, Moscow region, 142432 Russia.

Supporting information.

Table S1. IR spectra of starting compounds and complexes **1 – 4.**

Components	$Sn^{II}(Pc^{2-})$	$Sn^{II}(Nc^{2-})$	Cryptand $[M^+]$	$C_6H_4Cl_2$	$(Crypt[K^+])_2\{Sn(NC)_2Pc\}^{2-}\cdot C_6H_4Cl_2$ (**1**)	$(Crypt[K^+])_2\{Sn(CN)_2Nc\}^{2-}\cdot 4C_6H_4Cl_2$ (**2**)	$(Crypt[K^+])_2\{Sn(NCO)_2Pc\}^{2-}$ (**3**)	$(Crypt[Na^+])_2\{Sn(Im)_2Pc\}^{2-}\cdot 2C_6H_4Cl_2$ (**4**)
SnPc	435w	467m			441w	473w	-	442w
	627w	563w			-	565w 581w	-	-
	725m	709m			691s	707w	692s	691s
	745m	749s			743s*	752s*	744m*	750s*
	768m	844m			762m*	848w	-	766s
	819w	886m			820w	889w	-	820w
	872w	1013m			880w	1002w	-	879w
	887m	1025m			900w	1030m*	881w	901w
	948w	1080s			951s*	1081s*	951m*	941m
	1000w	1123w			-	1132s*	-	-
	1059s	1150w			1058s	1149w	1060s	1059s
	1072s	1199w			1079s*	1176w	1080s*	1077s*
	1114s	1213w			1131s*	1203m*	1133m*	1132s*
	1156w	1260m			-	1259m	-	1159w
	1283m	1319s			1263m	1315w	1262m	1258w
	1329s	1337s			-	1343s*	1353m*	-
	1407w	1358s			-	1354s*	1402w	1394m
	1454w	1464w			1445w	1455m*	1454m	1454s*
	1486s	1504w			1479w*	-	1481w*	-
					1529s	1510m	1531s	1530s
C-H	3049w	3050w			3049w	3047w	3046w	3048w
C-N vibrations					2219m	2199m	2194s	-
Cryptand$[M^+]$								
			476w		484m	486w	485w	484m
			528w		523w	522w	-	-
			581w		570w	565w*	-	-
			735m		743s*	752s*	744m*	742s
			922m		931m	932m	934w	928m
			948w		951s*	948s	951m*	941m
			982m		-	985w	-	985w
			1038w		-	1030m*	1048m	1034w*
			1071m		1079s*	1081s*	1080s*	1077s*
			1100s		1103vs	1102vs	1100vs	1100vs
			1127s		1131s*	1132s*	1133m*	1132s*
			1213w		1197w	1203m*	1200m	1199m
			1295m		1306m	1297m	1297m	1306s
			1329m		-	1343s*	1353m*	-
			1360s		1355m	1354s*	1361m	1356m
			1446m		1456m*	1443w	1443w	-
			1462m		-	1455m*	1466w	1454s*
			1490w		1479w*	1476m	1481w*	-
			2790w		2811w	2813w	2813w	2814w
			2877w		2873w	2880w	2890w	2864w
$C_6H_4Cl_2$			2943w		2956w	2950w	2971w	2962w
				657w	657w	657w	-	670w
				748s	762m*	752s*		750s*
				1030m	1030w*	1030m*		1034w*
				1122m	1131s*	1132s*		1132s*
				1453m	1456m*	1455m*		1454s*

w – weak, m-middle, s – strong, vs- very strong intensity; * - the bands coincide.

Spectra of KCN and KOCN in KBr pellets.[1] KCN has the position of the band associated with the CN vibrations at 2070 cm^{-1} whereas KOCN has the position of the band associated with the CN vibration at 2130 cm^{-1} and that associated with the CO vibrations at 1640 cm^{-1}.

[1] F. A. Miller, C. H. Wilkins, Infrared spectra and characteristic frequencies of inorganic ions. *Anal. Chem.*, **1952**, *24*, 1253–129

IR spectra of pristine compounds and compounds 1-4.

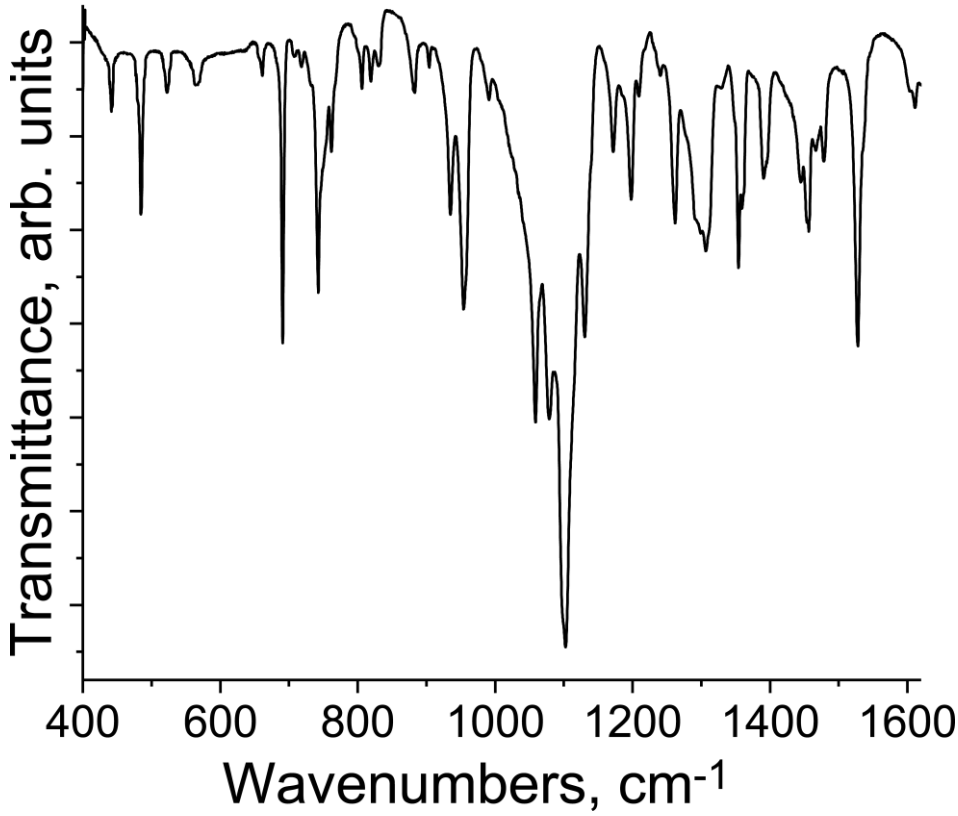

Fig. S1. IR spectrum of $(Crypt[K^+])_2\{SnPc(NC)_2\}^{2-}\cdot C_6H_4Cl_2$ (**1**) in KBr pellet prepared in the glove box.

.

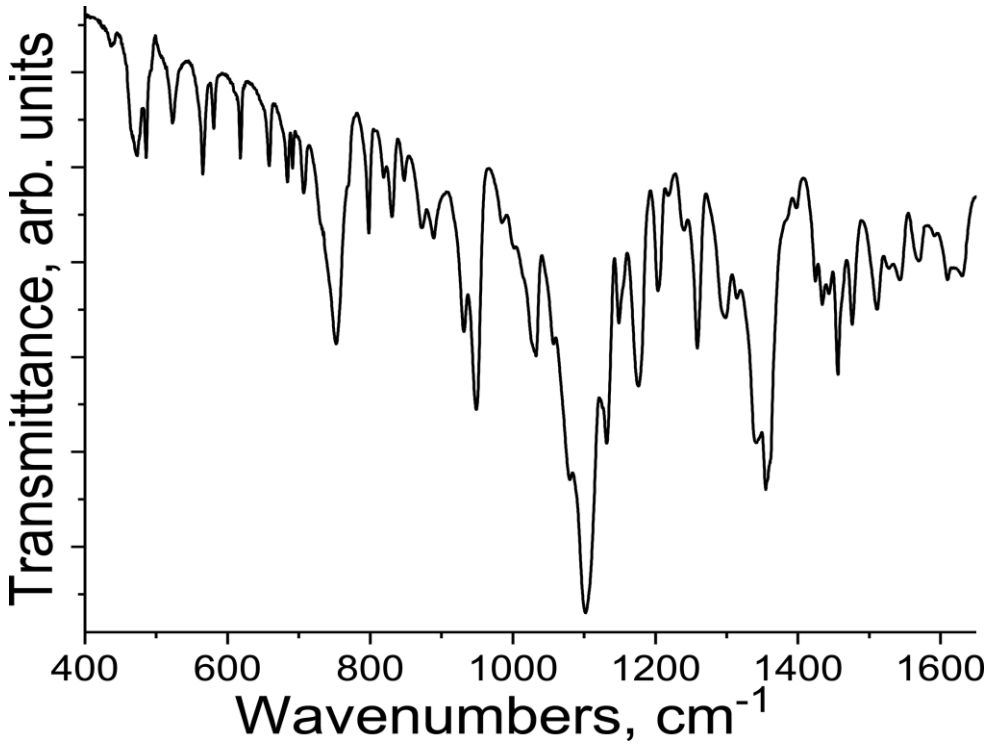

Fig. S2. IR spectrum of $(Crypt[K^+])_2\{SnNc(CN)_2\}^{2-}\cdot 4C_6H_4Cl_2$ (**2**) in KBr pellet prepared in the glove box.

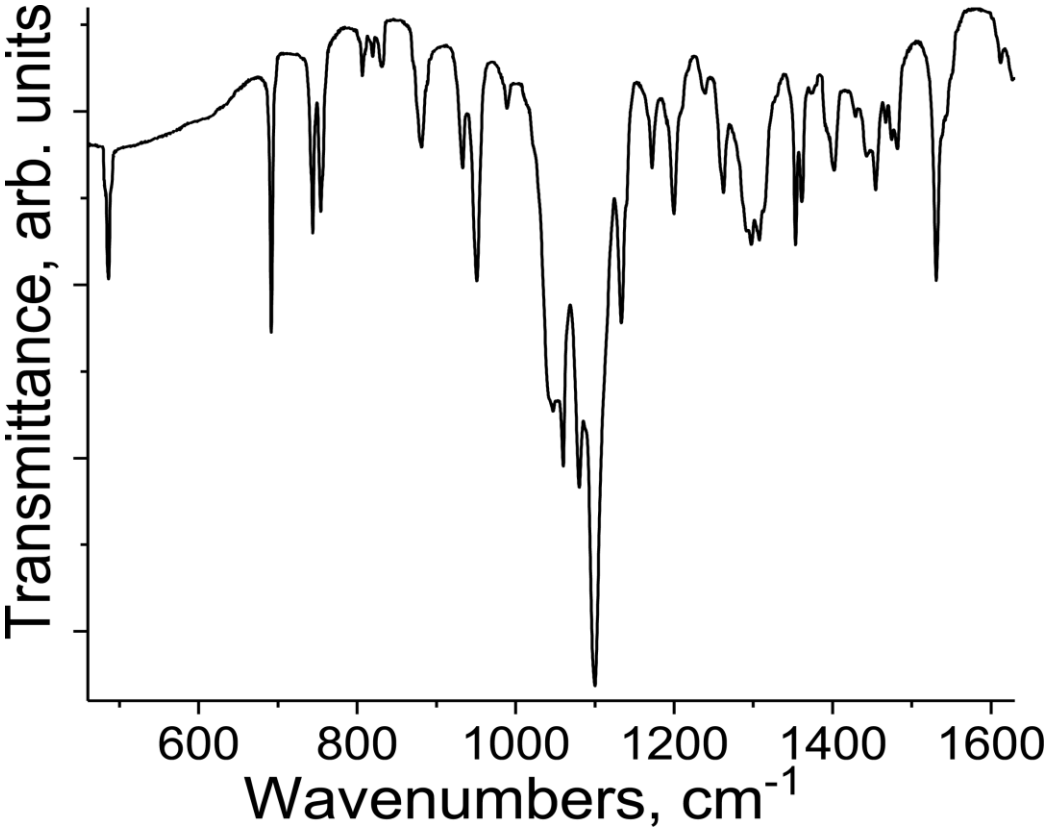

Fig. S3. IR spectrum of $(Crypt[K^+])_2\{SnPc(NCO)_2\}^{2-}$(**3**) in KBr pellet prepared in the glove box.

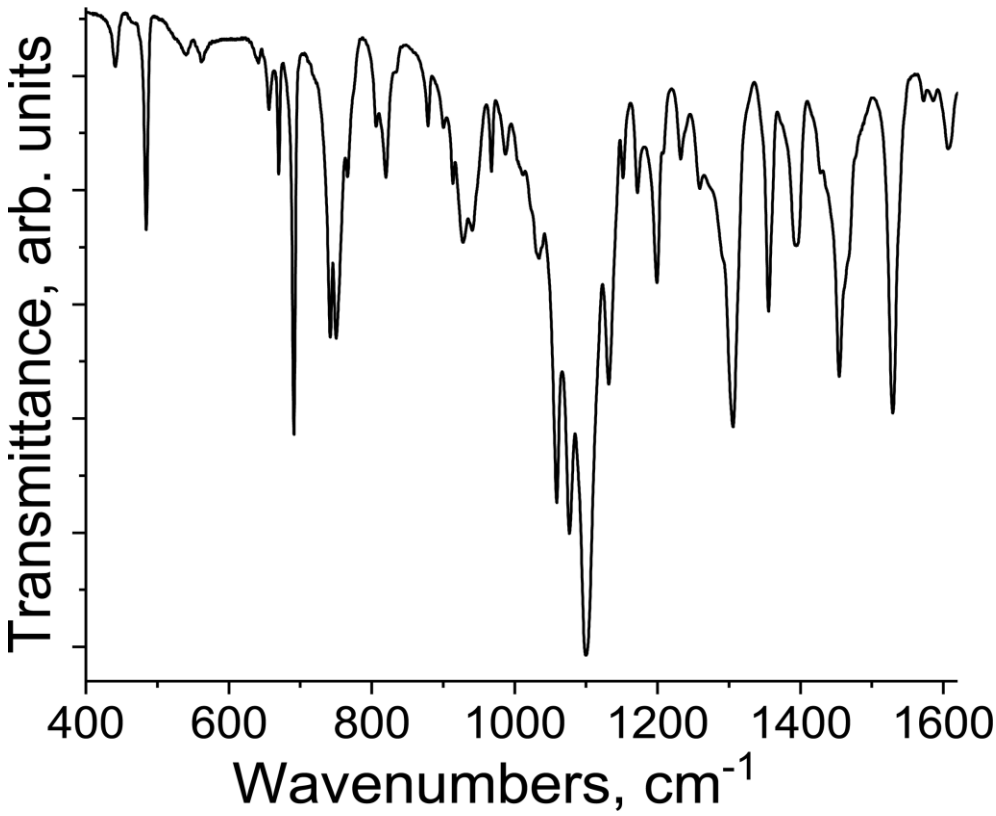

Fig. S4. IR spectrum of $(Crypt[Na^+])_2\{SnPc(Im)_2\}^{2-}\cdot 2C_6H_4Cl_2$ (**4**) in KBr pellet prepared in the glove box.

Crystal structures of complexes 3 and 4.

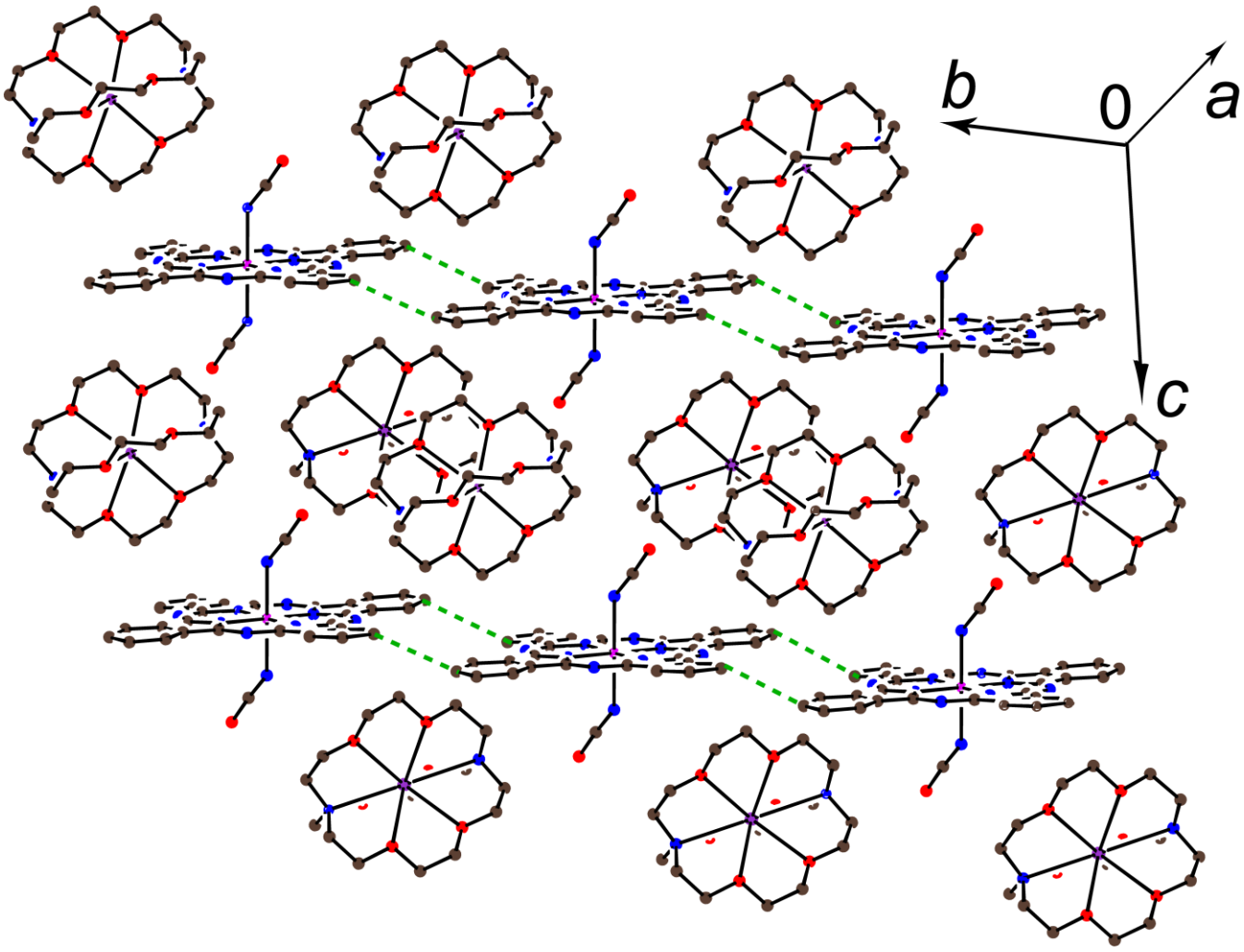

Fig. S5. View on two chains from the $\{Sn(NCO^{-})_2Pc\}^{2-}$ dianions in **3** and their surrounding from the crypt(K^+)} cations. The Van der Waals contacts between the macrocycles are shown by green dashed lines.

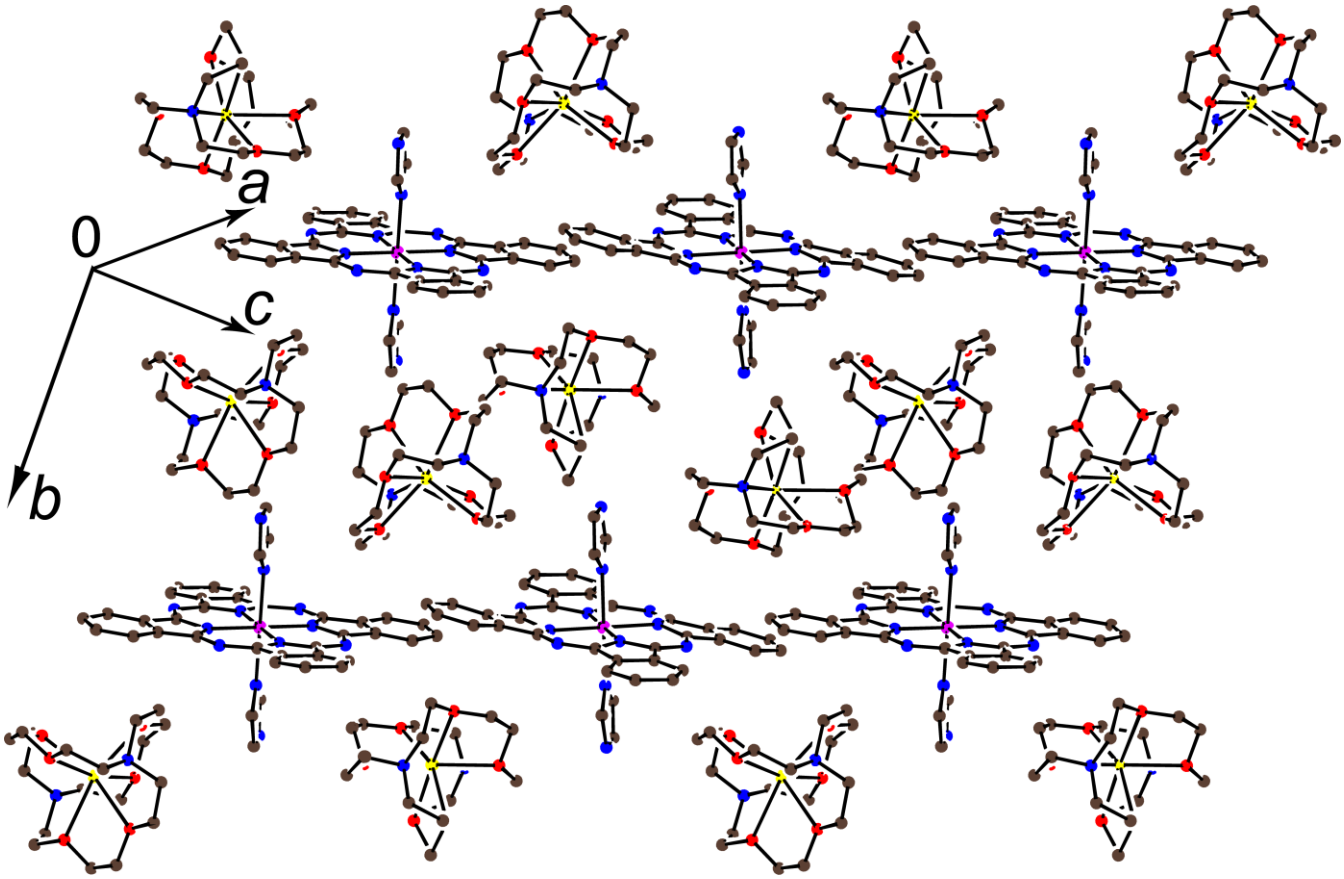

Fig. S6. View on two chains from the $\{Sn(Im^{-})_2Pc\}^{2-}$ dianions in **4** and their surrounding from the $\{crypt(Na^{+})\}$ cations.

Theoretical calculations.

For optimized structure $\{cryptand[2.2.2](K^+)\}_2\{Sn^{IV}(NC)_2(Pc^{4-})\}^{2-}$ (see Fig. 6 of the main text) theoretical IR spectrum shown in Fig. S7 was calculated. The IR spectra of the optimized structures $\{Sn^{IV}(NC)_2(Pc^{4-})\}^{2-}$ and $\{cryptand[2.2.2](K^+)\}_2$ are also given for comparison. Note that the presence of two cations leads to doubling of corresponding bands. In some cases low-intensity symmetrical stretching C-O vibrations of the isolated cation became very intensive in the complex due to their sensitivity to the strong Coulomb field of the counterion.

The effective masses and vibrational intensities are given in Table S2. For this simplest model complex, the structure of the theoretical IR spectrum agrees well with the experimental IR spectrum, namely four bands of middle intensity in the 400-600 cm^{-1} range, two intense bands in the range of about 700 cm^{-1}, double band at 930 cm^{-1}, and a very intense band of four superimposed peaks around 1100 cm^{-1} and series of bands of similar intensity: dual band below 1200 cm^{-1}, for bands in the 1250 -1400 cm^{-1} range, and a wide band with a fine structure at 1450 cm^{-1} and a narrow band at 1510 cm^{-1}.

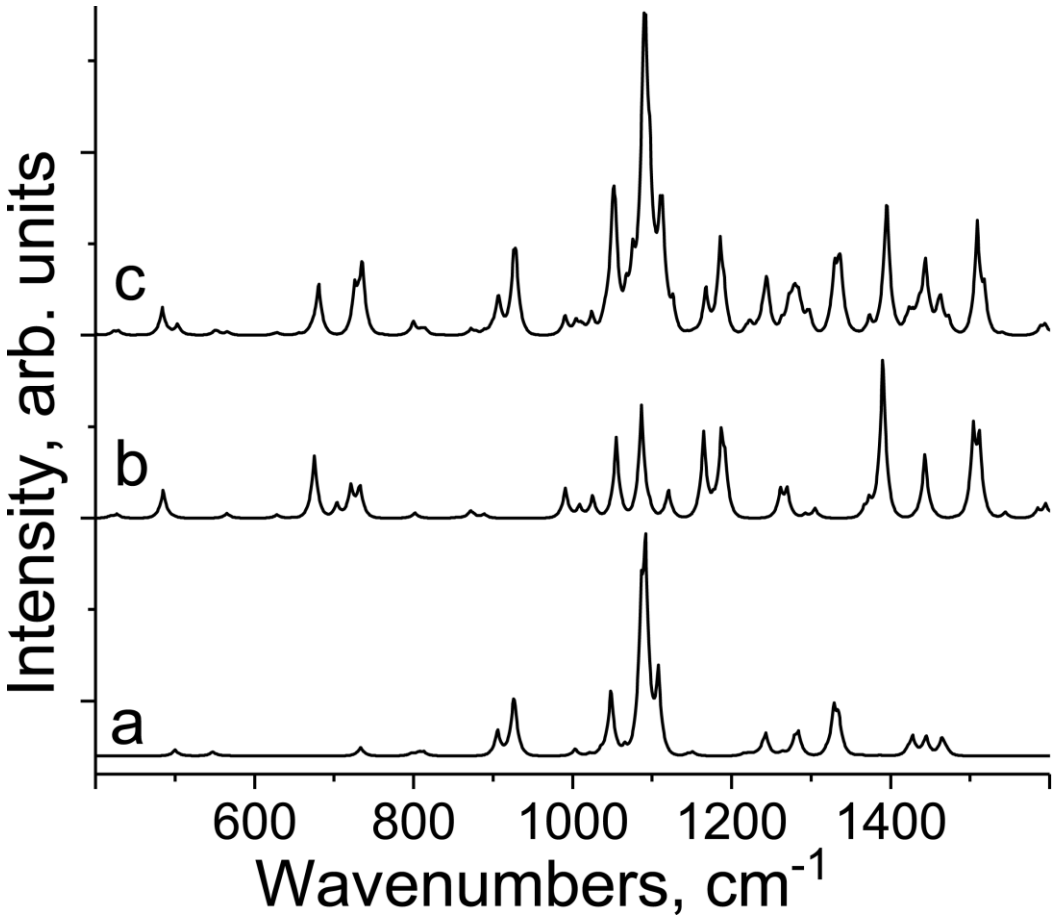

Fig. S7. Calculated IR spectra of the optimized structures of: (a) $\{cryptand[2.2.2](K^+)\}_2$; (b) $\{Sn^{IV}(NC)_2(Pc^{4-})\}^{2-}$ and (c) $\{cryptand[2.2.2](K^+)\}_2\{Sn^{IV}(NC)_2(Pc^{4-})\}^{2-}$.

Table S2

Most intense theoretical IR vibrations of the complex $\{cryptand[2.2.2](K^+)\}_2\{Sn^{IV}(Pc^{4-})(NC)_2\}^{2-}$ and its components.

$\{cryptand[2.2.2](K^+)\}_2$ $\{Sn^{IV}(Pc^{4-})(NC)_2\}^{2-}$			$\{Sn^{IV}(Pc^{4-})(NC)_2\}^{2-}$			$\{cryptand[2.2.2](K^+)\}$		
ν, cm^{-1}	μ, a.u.m	I, km/mol	ν, cm^{-1}	μ, a.u.m	I, km/mol	ν, cm^{-1}	μ, a.u.m	I, km/mol
428.9	3.41	11	427.1	3.45	10.4			
484	7.08	76.3	485.2	7.23	79.3			
503.1	2.23	15.5				500.1	2.16	17.2
503.4	2.32	11.9						
549.3	2.77	2.19				546.6	2.79	5.9
549.8	2.75	2.92						
550.8	2.78	3.6				548.1	2.80	5.9
551.9	2.78	3.96						
565.3	8.45	6.04	565.2	8.44	11.7			
680.6	4.42	148	675.3	2.85	182.0			
725.8	1.57	16.2	703.6	1.78	38.1			
726	1.6	97.5	721.3	1.55	55.8			
730.8	8.93	23.4	721.4	1.56	33.0			
730.8	5.38	4.13	731.2	9.65	34.1			
734.3	2.56	16.5				733.5	2.59	24.6
734.9	2.44	23.1						
735.4	2.77	36.3	733.2	9.18	58.7			
735.6	1.85	21.5						
735.8	1.75	94.2						
799	2	4.63				796.9	1.90	3.8
799.2	2.03	6.63						
799.6	2.25	7.3				798.4	1.90	3.9
800.1	2.92	10.6						
800.4	2.02	8.2				806.1	2.04	4.3
802	6.32	1.6	801.8	6.23	12.9			
809	2.02	1.6				807.8	2.05	5.2
809.3	2.03	6.2						
814.4	1.95	11				813.0	1.97	9.8
815	1.95	3.76						
872.2	9.66	17.3	871.6	9.85	17.8			
888.8	9.06	10.2	888.7	9.11	11.6			
905.8	2.16	29.2				905.4	2.19	36.7
906.2	2.16	31.8						
907.5	2.11	40				905.9	2.18	36.1
908.3	2.11	17.2						
925.9	2.03	129				925.6	2.07	102.0
927	2.02	9.72						
928	2.06	25.4				927.0	2.05	43.3

928.4	2.12	33.3						
928.7	2.07	25.8				928.0	2.06	38.4
929.2	2.01	81.8						
990.6	2.02	54.8	990.9	2.01	83.0			
1004.1	2.08	22.9				1003.4	2.08	19.9
1004.9	2.08	14.7						
1010.4	1.92	16.4	1008.8	1.93	35.1			
1023.7	2.9	14.4				1021.4	3.00	3.7
1024	2.94	13.5				1022.0	3.02	4.3
1024.3	8.1	32.4	1025.3	8.40	62.1			
1039.7	2.48	22.7				1035.5	2.71	7.7
1049.9	2.67	42.3				1036.0	2.74	5.6
1050.6	2.64	94.5				1048.2	2.65	58.6
1051	2.75	5.4				1048.3	2.71	34.6
1051.5	2.6	112						
1052.3	2.52	77.5				1048.5	2.62	94.9
1054.1	6.43	163	1055.0	5.98	224.3			
1067.1	3.73	36.4				1065.3	3.99	12.3
1067.5	3.76	31.3						
1068.5	3.77	17.6				1066.2	3.99	13.4
1068.6	3.72	18.7						
1075.5	4.23	149				1080.5	3.51	0.6
1076.9	4	41.1						
1081.2	3.83	5.1				1081.0	3.53	0.6
1082	3.75	10.5						
1086.7	3.26	95.3				1086.6	4.61	333.5
1089.1	3.84	96.4						
1089.8	2.13	370	1086.8	1.72	320.9			
1091.5	2.64	119				1091.7	4.44	484.4
1091.9	2.59	92.6						
1092.1	2.48	143				1093.9	2.46	24.9
1093.3	2.51	126						
1097.1	3.13	160				1095.0	2.34	16.7
1097.8	3.54	111						
1109.4	4	15.5				1107.8	5.66	114.4
1110.1	4.5	171						
1112.7	4.76	48.2				1108.0	5.68	114.6
1112.9	4.75	175						
1126.4	1.44	85.2	1120.6	1.35	80.9			
1167.6	2.49	135	1165.0	2.79	236.3			
1185.7	2.6	251	2.70	206.7				
1190.6	2.63	75.3	1191.9	2.71	113.3			
1242.1	1.18	11.7				1243.2	1.21	31.5
1243.4	1.2	67.6						
1244.7	1.18	67.5				1243.5	1.22	22.3
1246	1.21	18.7						
1271.7	1.77	62.1				1278.6	1.22	17.2
1274.4	1.23	18.3						

1277.5	1.2	25				1279.3	1.22	17.1
1277.9	1.2	24.2						
1284.2	1.15	31.2				1284.2	1.13	49.5
1284.7	1.15	34.2						
1288	1.16	12.6	1261.6	3.70	73.4			
1295.2	2.88	29.8	1269.8	1.76	74.6			
1298.2	8.62	44.9	1304.9	9.12	27.1			
1329.3	1.22	84				1328.6	1.21	117.9
1329.9	1.22	69.8						
1334.4	1.29	70				1333.5	1.26	49.8
1336.4	1.3	66.5						
1337.4	1.26	64.1				1335.5	1.27	50.2
1337.8	1.26	23.8						
1373.6	3.08	38.2	1366.8	3.10	21.2			
1393.5	3.59	84.9	1373.2	7.00	44.8			
1395.6	6.35	314	1390.3	7.15	457.5			
1422.8	1.11	12.6				1421.6	1.10	5.5
1423	1.11	11.4						
1423.6	1.12	13.3				1422.6	1.09	4.4
1423.6	1.12	13.6						
1427.6	1.14	17.4				1427.8	1.12	49.9
1427.9	1.13	11.5						
1442.4	1.09	15.6				1444.4	1.09	13.2
1443.5	1.13	25.6						
1443.9	2.77	136	1443.2	3.28	181.9			
1446.5	1.1	10.2				1445.4	1.09	23.2
1447.7	1.1	11.7						
1460.3	1.1	20.1				1463.7	1.09	20.9
1460.5	1.11	6.75						
1462.4	1.18	24.4				1465.0	1.09	15.2
1462.7	1.52	15.3						
1463.8	1.1	7.76				1466.6	1.09	11.3
1464.1	1.11	22						
1472.6	1.09	20.8				1470.4	1.09	10.7
1473.4	1.09	20.4						
1509	10.4	298	1504.2	10.30	231.0			
1518	10.7	105	1511.8	10.79	200.5			
1594.5	7.21	26.1	1585.1	7.16	23.1			
1613.6	7.61	49.9	1594.9	7.27	35.2			

The structure of complex $\{cryptand[2.2.2](K^+)\}_2\{Sn^{IV}(NC)_2(Pc^{4-})\}^{2-}$ with opposite coordination of the CN ligands by carbon atom was investigated as well. The restricted optimization with the imposed condition that the Sn-K distances coincide with their values in a real crystal structure, 9.145 and 9.151 Å gives the longest Sn-C(CN) bond has the value of 2.380 Å (as the longest Sn-N(CN) bond in **1**). But its elongation 0.104 Å (see Table 3 in the manuscript) is about two times less than in the case of the *N*-coordinated CN ligand, 0.187 Å. In view of the same fixed Sn-K distances this difference is due to smaller charge on the CN ligand in a free dianion and a stronger Sn-C(CN) bond.

In isomeric centrosymmetrical complex $\{cryptand[2.2.2](K^+)\}_2\{Sn^{IV}(NC)_2(Pc^{4-})\}^{2-}$ with the opposite orientation of the cations with respect to the Sn atom some part of macrocycle is located in the region where electric fields of the cations mainly cancel each other. For the optimized structure with the fixed Sn-K distances at 9.151 Å the cations have practically the same total charge 1.55+. But macrocycle charge, 1.32–, changes only slightly, and the main part of the charge transfer (85%) is originated from the NC ligands. In this case the NC ligands are also strongly affected by Coulomb field of the cations. However, this effect is smaller than that in the case of the isomeric complex shown in Fig. 6 where one NC ligand has two cation neighbors. That is why Sn-N(CN) bond length after elongation is only 2.216 Å in centrosymmetrical complex. This example illustrates well how important is peculiarities of the cationic surroundings.

For that purpose experimental crystal structures of **1**, **2** and **3** were analyzed. The arrangement of the nearest cations around the $\{Sn^{IV}L_2Pc\}^{2-}$ dianions (L = NC, NCO) is shown in Fig. S8.

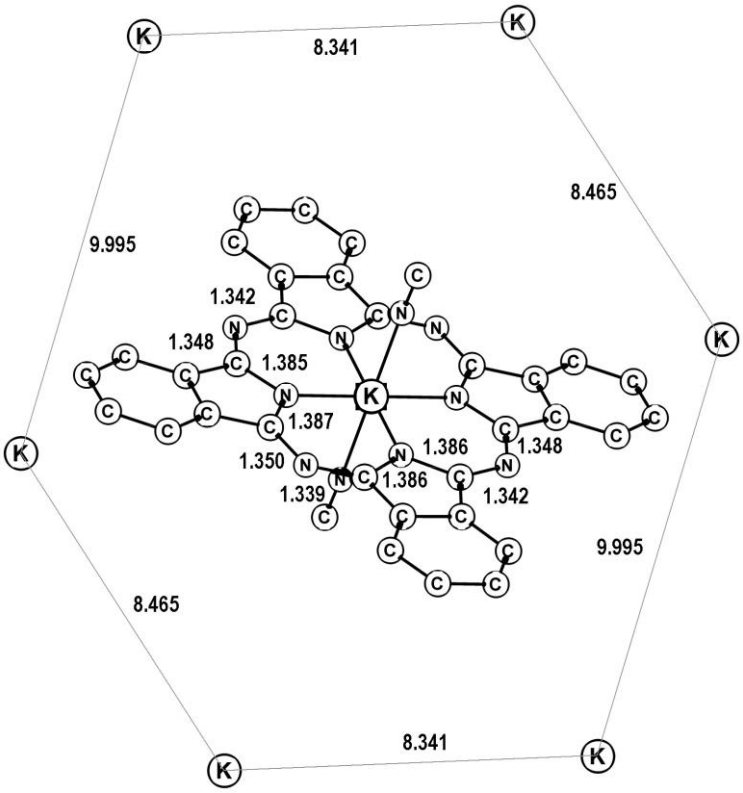

a

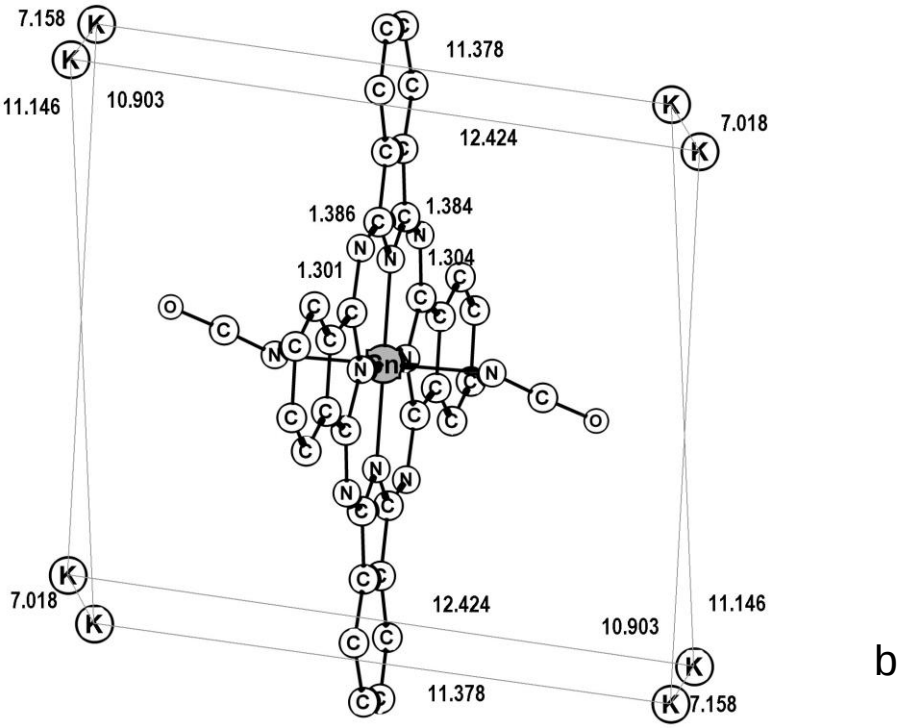

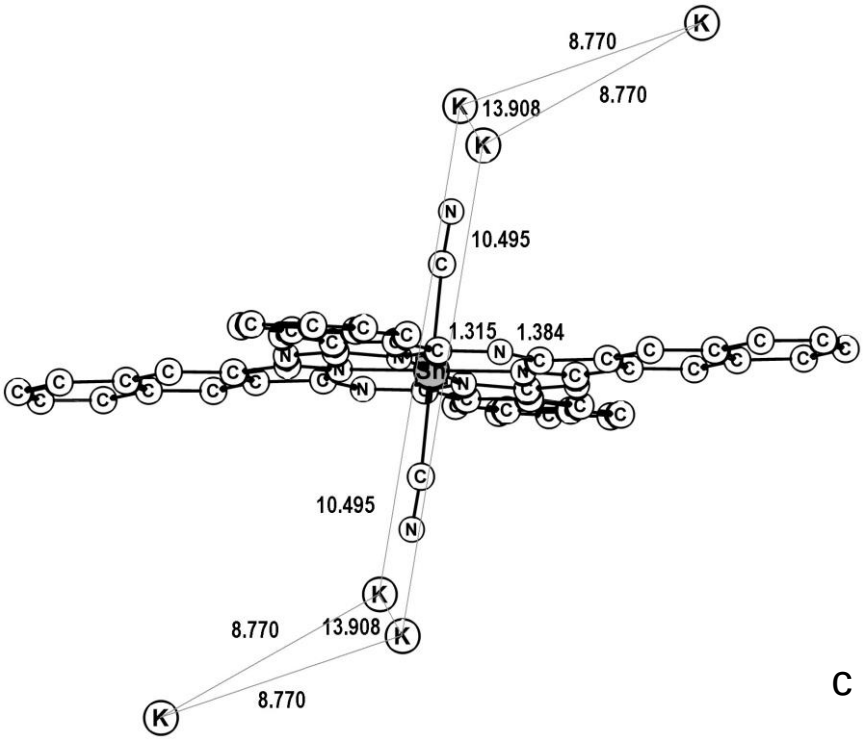

Fig. S8. The arrangement of the nearest cations in the structures of $\{Sn^{IV}(NC)_2Pc\}^{2-}$ in **1** (a); $\{Sn^{IV}(NCO)_2(Pc^{4-})\}^{2-}$ in **3** (b); and $\{Sn^{IV}(CN)_2(Nc^{4-})\}^{2-}$ in **2** (c).

The chosen projections show the orientation of the macrocycle plane relative to pseudosymmetry plane of polyhedron composed from K^+ cations. The mean Sn – K distance of 8.85 Å is the same for the $\{Sn^{IV}(NC)_2Pc\}^{2-}$ and $\{Sn^{IV}(NCO)_2Pc\}^{2-}$ dianions. However, the structure of a distorted cube from the eight countercations around the dianions and their orientation relative to them is different. In the structure of **2** (Fig. S8c), a trigonal distortion of a regular cube occurs (flattening of a ring of six cations around the C_3 axis). At the same time, the cube from the surrounding countercations turns to the pseudo-parallelepiped in the structure of **3** (Fig. S8b). As a result, in complexes **2** and **3**, both the macrocycles and the ligands are exposed to approximately the same uniform fields from each counterion due to close Sn-K distances. However, due to the specific arrangement of cations in **3**, these fields effectively quench each other since the macrocycle is located in a plane approximately equidistant from the nearest cations. On the contrary, in the structure of **1** (Fig. S8a), both axial ligands and a part of macrocycle atoms are exposed to an uncompensated electric field from the nearest cation near the axis of trigonal distortion. In fact, the oppositely directed forces act on the oppositely located N_{im} atoms and cause the alignment of the C-N_{im} bonds. In the structure **2** with $\{Sn^{IV}(CN)_2(Nc^{4-})\}^{2-}$, the increased mean Sn-K distance of 8.91 Å is realized. Similar to the structure of **3**, the axial ligands are approximately equidistant from the cations and are not affected by the electric field. The macrocycle plane is approximately perpendicular to the plane in which the nearest counterions are located, and forms a small angle with the planes passing through the top and bottom triangle of the K^+ ions. For this reason, the greatest effect of the electrical field is observed in the direction peripheral to the phenylene substituents of Pc.

Theoretical spectra in the UV-visible-NIR range obtained from the TDDFT calculations.

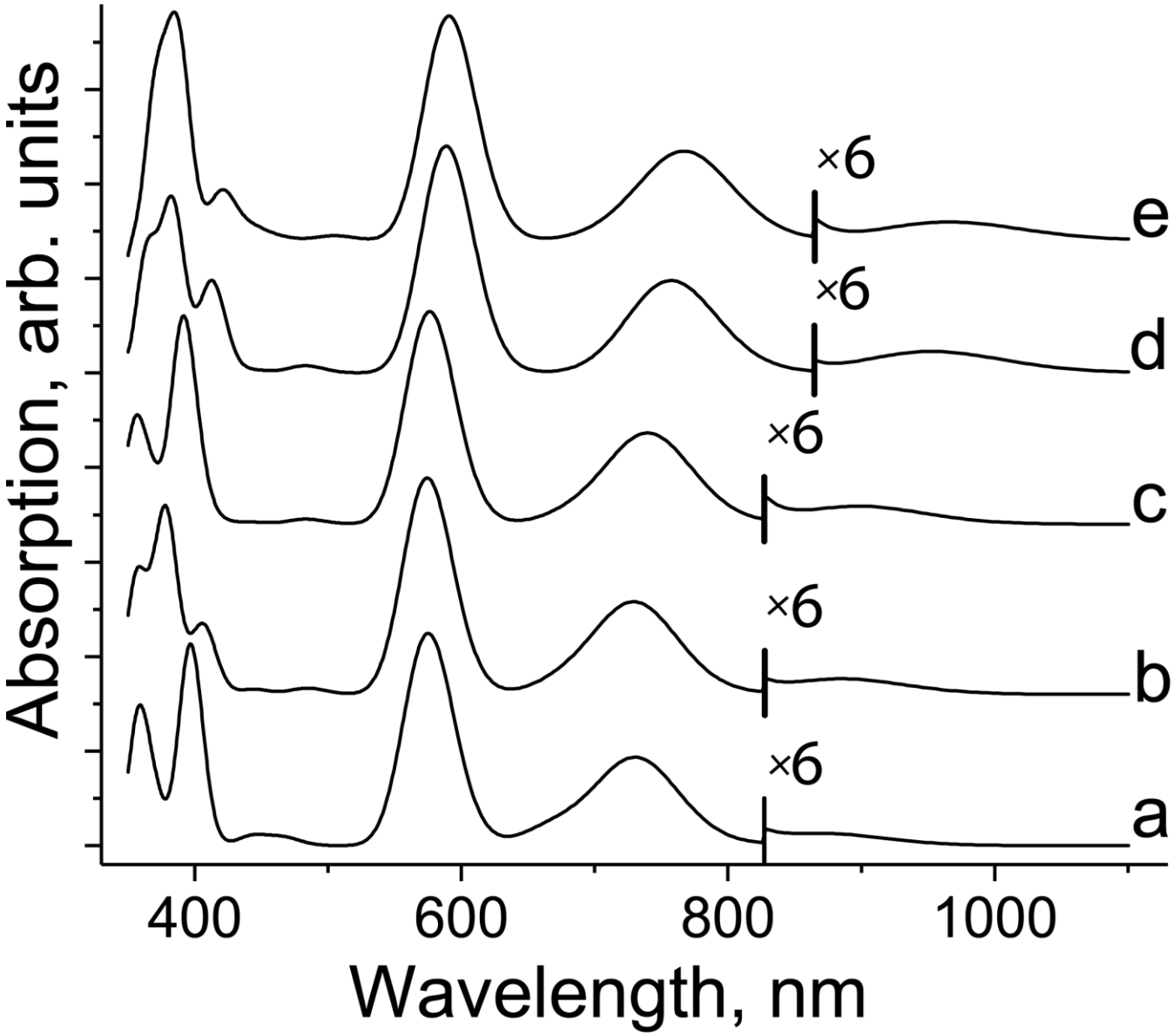

Fig. S9. Spectra of the theoretical structures according to the TDDFT calculations. Isolated dianions with alternating bonds for: (a) $\{Sn^{IV}(NC)_2(Pc^{4-})\}^{2-}$, (b) $\{Sn^{IV}(CN)_2(Pc^{4-})\}^{2-}$ and (c) $\{Sn^{IV}(NCO)_2(Pc^{4-})\}^{2-}$; (d) the $\{Sn^{IV}(NC)_2(Pc^{4-})\}^{2-}$ dianion with the same geometry of the macrocycle as in the $\{Sn^{IV}(NC)_2(Pc^{\bullet 3-})\}^{\bullet -}$ radical anion but larger alignment of the bonds; (e) the $\{Sn^{IV}(NC)_2(Pc^{4-})\}^{2-}$ dianion with the lengths of the C-N_{im} and C-N_{py} bonds fixed as in the experimental structure.